JOURNAL OF BACTERIOLOGY, May 1999, p. 3201–3211 Vol. 181, No. 10
0021-9193/99/$04.00+0


# Septal Localization of Penicillin-Binding Protein 1 in *Bacillus subtilis*

LOTTE B. PEDERSEN,[1] ESTHER R. ANGERT,[2] AND PETER SETLOW[1]*

*Department of Biochemistry, University of Connecticut Health Center, Farmington, Connecticut 06032,[1] and Department of Molecular and Cellular Biology, The Biological Laboratories, Harvard University, Cambridge, Massachusetts 02138[2]*

Received 30 November 1998/Accepted 26 February 1999

**Previous studies have shown that *Bacillus subtilis* cells lacking penicillin-binding protein 1 (PBP1), encoded by *ponA*, have a reduced growth rate in a variety of growth media and are longer, thinner, and more bent than wild-type cells. It was also recently shown that cells lacking PBP1 require increased levels of divalent cations for growth and are either unable to grow or grow as filaments in media low in $Mg^{2+}$, suggesting a possible involvement of PBP1 in septum formation under these conditions. Using epitope-tagging and immunofluorescence microscopy, we have now shown that PBP1 is localized at division sites in vegetative cells of *B. subtilis*. In addition, we have used fluorescence and electron microscopy to show that growing *ponA* mutant cells display a significant septation defect, and finally by immunofluorescence microscopy we have found that while FtsZ localizes normally in most *ponA* mutant cells, a significant proportion of *ponA* mutant cells display FtsZ rings with aberrant structure or improper localization, suggesting that lack of PBP1 affects FtsZ ring stability or assembly. These results provide strong evidence that PBP1 is localized to and has an important function in the division septum in *B. subtilis*. This is the first example of a high-molecular-weight class A PBP that is localized to the bacterial division septum.**

The bacterial peptidoglycan is composed of glycan strands with peptide side chains which cross-link the glycan strands to each other. During growth, new disaccharide pentapeptide units become inserted into the existing peptidoglycan by the penicillin-binding proteins (PBPs) (17, 23, 36, 37). PBPs can be divided into three groups: low-molecular-weight PBPs and class A and class B high-molecular-weight (HMW) PBPs (17). Low-molecular-weight PBPs are usually monofunctional DD-carboxypeptidases, which are involved in regulating the number of peptide cross-links (17). Class A HMW PBPs possess both transglycosylase and transpeptidase activities (24, 55) and are somewhat functionally redundant (26, 46), while class B HMW PBPs are monofunctional transpeptidases, some of which have essential functions in cell septation and regulation of cell shape (1, 17, 18, 38).

During cell growth rod-shaped bacteria display two modes of peptidoglycan synthesis: elongation and septation (23, 36, 37). For *Escherichia coli*, it is widely assumed that the class B HMW PBP2 is involved in elongation while the class B HMW PBP FtsI (also known as PBP3) is needed for septation (38, 53, 61). Homologues of PBP2 and FtsI are also found in *Bacillus subtilis* (34, 62). Since class B HMW PBPs have no transglycosylase activity (1, 17, 57), these proteins cannot synthesize peptidoglycan. Therefore, it has been proposed that the class A HMW PBPs synthesize and to some extent cross-link primers, which are then used by class B HMW PBPs during septation and elongation (61). This model is supported by studies using specific inhibitors of the major *E. coli* class A HMW PBPs (61) and by affinity chromatography studies, which indicate that the *E. coli* class A HMW PBPs PBP1a and PBP1b interact either directly or indirectly with the class B HMW PBPs PBP2 and FtsI (23). In addition, genetic studies have shown that *E. coli* PBP1b is a possible helper protein for FtsI (15), and antibiotic inhibition studies have indicated that triggering of cell lysis by inhibitors of PBP1a and PBP1b in *E. coli* is linked to cell division (16), suggesting a role for class A HMW PBPs in cell division. Recent evidence from our laboratory suggests that in growth media low in $Mg^{2+}$ the class A HMW PBP1 may also play a role in cell division in *B. subtilis*, because cells lacking PBP1 sometimes grow as filaments (35). PBP1, encoded by *ponA*, is expressed predominantly during vegetative growth, and mutants lacking PBP1 have a reduced growth rate in a variety of growth media (45, 46). Although vegetative *B. subtilis* cells contain two other class A HMW PBPs (PBP2c and PBP4) (43, 44), PBP1 appears to be functionally more important than PBP2c and PBP4 (35, 46).

In addition to PBPs, septum formation in *E. coli* requires the concerted action of the division proteins FtsZ, FtsA, FtsK, FtsL, FtsN, FtsQ, FtsW, and ZipA, which are believed to form a complex at the division site, called the divisome (10, 37, 48), whose key component is the FtsZ ring (9, 48). Except for FtsL, the other Fts proteins as well as ZipA have now been localized to the division site in *E. coli* (2–4, 11, 19, 31, 58–60, 64); in *B. subtilis* the division proteins DivIB (an FtsQ homologue), DivIC, and FtsZ have also been localized to division sites (21, 25, 31). However, no class A HMW PBPs have been demonstrated to localize to division sites in either organism, although immunoelectron microscopy showed that PBP1b from *E. coli* is present in higher amounts around inner membrane-outer membrane contact areas than in other parts of the cell (7).

In this communication, we report studies of the subcellular localization of PBP1 in exponentially growing *B. subtilis* cells using immunofluorescence microscopy; these studies show that PBP1 localizes to division sites.

* Corresponding author. Mailing address: Department of Biochemistry, University of Connecticut Health Center, 263 Farmington Ave., Farmington, CT 06032. Phone: (860) 679-2607. Fax: (860) 679-3408. E-mail: setlow@sun.uchc.edu.

TABLE 1. PCR primers used in this study

| Primer | Nucleotide sequence[a] |
|---|---|
| ponAP1 | 5′-CCGGAATTCCGGCAGCTACTCCG-3′ |
| ponAP2 | 5′-CGCGGATCCGACCCAATACC-3′ |
| ponAP3 | 5′-CCATTGAAAAAACAAAT**GACTACAAGGACCACGATGACAAG**TAAACAAAAAAGCCG-3′ |
| ponAP4 | 5′-GGGAATGGGAGAAAAC-3′ |
| pFLAG | 5′-**GACTACAAGGACGACGATGACAAG**-3′ |
| p1219 | 5′-ATGCGTCCGGCGTAGA-3′ |

[a] Restriction endonuclease sites are underlined; nucleotides encoding the FLAG epitope are shown in bold.

## MATERIALS AND METHODS

***B. subtilis* strains, recombinant plasmids, and growth conditions.** All *B. subtilis* strains used are derivatives of PS832, a prototrophic revertant of strain 168. Transformation of *B. subtilis* was as described previously (6), and transformants were selected on 2× SG (30) agar plates with chloramphenicol (Cm; 5 μg/ml). Strain PS2062 carrying a spectinomycin resistance (100 μg/ml) cassette ($Sp^r$) in the *ponA* gene (*ponA*::$Sp^r$) has been described previously (45). Strain LP27 was generated by transformation of PS832 with plasmid pLP3 (see below), resulting in integration of pLP3 into the chromosome by a single crossover event at the 3′ end of the coding region of *ponA*. Therefore, strain LP27 contains a 24-bp DNA sequence encoding the FLAG epitope immediately before the stop codon of the *ponA* gene, followed by a Cm resistance marker and the sequence corresponding to the 3′ noncoding region of *ponA*. Routinely, cells were grown at 30 or 37°C overnight on 2× SG agar plates with or without appropriate antibiotics, inoculated into 20, 50, or 100 ml of 2× YT medium (containing [per liter] 16 g of tryptone, 10 g of yeast extract, 5 g of NaCl) or Penassay broth with no antibiotics, and grown at 30 or 37°C.

**Plasmids and epitope tagging.** Plasmid pDPC273 was a gift from David L. Popham (Virginia Polytechnic Institute, Blacksburg, Va.). It is a derivative of plasmid pJH101 (14), which contains an ~3.8-kb insert comprising the region from the *Hin*dIII site in the gene upstream of *ponA* (*prfA*) to the *Eco*RV site downstream of *ponA* (45). For tagging of PBP1 with the FLAG epitope, a megaprimer PCR-based method (49) was used. All oligonucleotides were purchased from GIBCO and are listed in Table 1. All PCRs were carried out with *Thermus aquaticus* DNA polymerase (GIBCO). The first round of PCR was carried out by using the primers ponAP2 and ponAP3 with chromosomal DNA from strain PS832 as a template and gave a 215-bp product corresponding to the region from nucleotide (nt) 4050 to nt 4234 of the *ponA* operon (45) plus 24 bp encoding the FLAG epitope. The 215-bp PCR product was purified by using a PCR purification kit (QIAGEN) and used as a megaprimer in a second round of PCR with ponAP1 used as the upstream primer and linearized pDPC273 plasmid DNA used as the template. The product of the second round of PCR (720 bp), corresponding to the region from nt 3553 to nt 4234 of the *ponA* operon (45), was ligated into pCR2.1 (Invitrogen), and after transformation into *E. coli* INVαF′ competent cells (Invitrogen), plasmids were prepared and the inserts were sequenced by using an automated DNA sequencer. A plasmid with an insert whose sequence was as expected was digested with *Eco*RI and *Bam*HI, and the 712-bp insert was ligated into plasmid pJH101 (14) digested with the same enzymes to generate plasmid pLP3, which was used to transform *B. subtilis* to Cm resistance. Transformants were screened by PCR using primers ponAP4 and p1219, and pFLAG and p1219, respectively.

**Membrane preparation, penicillin-binding assay, SDS-PAGE, and Western blot analysis.** Cells from 50- or 100-ml log-phase cultures (optical density at 600 nm [$OD_{600}$] of ~0.5) grown in 2× YT medium were harvested by centrifugation (7,000 × *g*, 10 min), washed with 5 ml of wash buffer (50 mM Tris [pH 8], 1 mM $MgCl_2$, 1 M KCl, 1 mM phenylmethylsulfonyl fluoride [PMSF]), resuspended in 0.7 ml of buffer A (100 mM Tris-HCl [pH 8], 1 mM $MgCl_2$, 1 mM β-mercaptoethanol [β-ME], 1 mM PMSF) containing 285 μg of lysozyme/ml, and incubated on ice for 20 min. Cells were broken by sonication in the presence of glass beads, the lysate was cleared by centrifugation (20,000 × *g* for 15 min at 4°C), and membranes were pelleted by centrifugation at 100,000 × *g* for 1 h at 4°C. The supernatant fluid from the latter step was stored at −20°C and used for DNA quantitation. The membranes were washed with 1 ml of buffer B (50 mM Tris-HCl [pH 8], 1 mM β-ME, 1 mM PMSF), resuspended in 90 μl of buffer B, and stored at −80°C. Membranes were incubated with fluorescein-hexanoic acid-6-aminopenicillanic acid (FLU-C6-APA) and assayed for penicillin-binding activity as previously described (46). For Western blotting, different amounts (10 to 40 μg) of crude membrane protein in 10 μl of buffer B were mixed with 10 μl of 2× sodium dodecyl sulfate (SDS) sample buffer (29) and boiled for 4 min, and proteins were separated by SDS–10% polyacrylamide gel electrophoresis (PAGE). Various amounts (9.4 to 600 ng) of C-terminal FLAG-bacterial alkaline phosphatase (BAP) (Sigma) were loaded on the same gels to serve as a standard for quantitative Western blotting. After electrophoresis the proteins on SDS gels were transferred to Immobilon-$P^{sq}$ membranes (Millipore) in transfer buffer (3 g of Tris base/liter, 14.4 g of glycine/liter, 20% methanol [vol/vol], 0.08% [wt/vol] SDS), and the membranes were subjected to immunoblotting as described below.

**Immunoblotting and protein and DNA quantitation.** Immunoblotting was carried out essentially as in the protocol for the BM Chromogenic Western blotting kit (Boehringer). The primary antibody was anti-FLAG M2 monoclonal antibody (4 μg/ml) (Sigma). The secondary antibodies were a commercially available mixture of goat anti-mouse immunoglobulin G (IgG) and goat anti-rabbit IgG, both conjugated to alkaline phosphatase (1:2,000 dilution) (Boehringer). The blots were scanned, and the relative FLAG content of each band was determined by using an IS-1000 digital imaging system and software from Alpha Innotech Corporation. Protein concentrations were determined by the Lowry procedure (32) by using bovine serum albumin (BSA) as the standard. DNA quantitation was performed with the Hoechst 33258-based fluorescent DNA quantitation kit (Bio-Rad) by using calf thymus DNA (Bio-Rad) as a standard. Calf thymus DNA has about the same A+T content (58%) as *B. subtilis* DNA (56.5% [28]), and hence is appropriate to use as a standard in this assay.

**Preparation of cells for immunofluorescence microscopy.** For FLAG localization, cells were grown at 37°C in 2× YT medium to an $OD_{600}$ of ~0.5 and prepared for immunofluorescence microscopy as described previously (20, 41) with modifications. Briefly, cells were fixed for 20 min at room temperature in 4.4% (wt/vol) paraformaldehyde–28 mM $NaPO_4$ (pH 7), washed three times with phosphate-buffered saline (PBS; containing [per liter] 8 g of NaCl, 0.2 g of KCl, 1.44 g of $Na_2PO_4$, 0.24 g of $KH_2PO_4$ [pH 7.4]), resuspended in 100 μl of GTE (50 mM glucose, 20 mM Tris-HCl [pH 7.5], 10 mM EDTA), treated with lysozyme (2 mg/ml) for 30 to 60 s at room temperature, washed twice with PBS, resuspended in 70 μl of PBS, and applied to poly-L-lysine-coated microscope slides. The excess cell suspension was removed, and the slides were washed two times with PBS and allowed to dry completely. After rehydration with PBS, the slides were blocked for 20 min at room temperature with 2% (wt/vol) BSA in PBS and incubated for 2.5 h at room temperature in PBS containing 10 μg of anti-FLAG M2 monoclonal antibody/ml and 0.1% (wt/vol) BSA. The slides were washed six times with PBS and incubated overnight at 4°C in PBS containing a 1:100 dilution of biotinylated goat anti-mouse IgG (Molecular Probes) and 0.1% (wt/vol) BSA. Slides were subsequently washed six times with PBS and incubated for 2 h at room temperature with PBS containing 0.1% (wt/vol) BSA and 5 μg of indocarbocyanine (Cy3)-conjugated streptavidin (Jackson ImmunoResearch Laboratories) per ml. After being washed six times with PBS, the slides were mounted by using the SlowFade antifade kit from Molecular Probes.

For FtsZ localization, cells were grown as described above and fixed by adding 1 ml of cell culture to 10 ml of cold (−20°C) 80% methanol as described (22) with modifications. After fixing for 1 h at room temperature, 200 μl of 16% (wt/vol) paraformaldehyde was added to the cell suspension, and after a 5-min incubation at room temperature, cells were pelleted by centrifugation at 3,000 × *g* for 15 s at room temperature, the supernatant was discarded, and cells were gently resuspended in the residual fluid by tapping the tube. Then 1 ml of 80% methanol was added, and the cells were spun gently as described above, the supernatant was removed, and the pellet was resuspended in GTE. Lysozyme was added to 2 mg/ml, and the cells were placed on poly-L-lysine-coated microscope slides and incubated at room temperature for 30 to 60 s. Excess cell suspension was removed, and the slides were washed, dried, rehydrated and blocked with BSA as described for FLAG localization, and incubated for 2 h at room temperature with a 1:500 dilution of affinity-purified rabbit antiserum against *B. subtilis* FtsZ (a gift from Petra A. Levin, Massachusetts Institute of Technology, Cambridge, Mass.) in PBS containing 2% (wt/vol) BSA. After being washed 10 times with PBS, the slides were incubated for 2 h with 3.75 μg of Cy3-conjugated donkey anti-rabbit serum (Jackson ImmunoResearch Laboratories) per ml in PBS containing 2% (wt/vol) BSA, washed 10 times with PBS, and mounted for microscopy as for cells stained for the FLAG epitope.

**Staining of cell walls and nucleoids.** For staining of cell walls and/or nucleoids of immunostained cells, 2 μg of 4′,6′-diamidino-2-phenylindole (DAPI) (Sigma) per ml and/or 2 μg of Oregon green- or fluorescein isothiocyanate (FITC)-conjugated wheat germ agglutinin (WGA) (Molecular Probes) was included in the Cy3 mix. (WGA is a lectin that binds to oligomers of *N*-acetylglucosamine and *N*-acetylmuramic acid and has been found to bind well to lysozyme-treated cell walls of *B. subtilis* [5, 42, 52].) For cell wall and nucleoid staining only, cells grown in 2× YT medium at 30 or 37°C were treated like cells stained for the FLAG epitope except that incubations with antibodies and streptavidin were omitted and the slides were incubated for 2 h at room temperature with PBS containing 0.1% (wt/vol) BSA, 0.2 μg of DAPI/ml, and 2 μg of Oregon green-

WGA/ml before the final PBS wash. In some cases, propidium iodide (10 μg/ml) was used instead of DAPI to visualize RNA, DNA, and septa (31).

**Fluorescence microscopy and image analysis.** Cells (see Fig. 3) were visualized with a Zeiss Axiovert 100 fluorescence microscope equipped with a 63× Plan-NEOFLUAR immersion lens (Zeiss) and a standard filter block for visualizing Cy3 and Oregon green; images were captured with a cooled charge-coupled device camera by using exposure times of 700 (Cy3) or 500 (Oregon green) ms. Fluorescence microscopy of cells (see Fig. 4 and 7) was performed with an Olympus BX60 microscope equipped with a 100× UPlanFluor objective and standard filter sets for visualizing DAPI, Cy3, and Oregon green or FITC; images were captured with a MicroMax (Princeton Instruments)-cooled charge-coupled device camera driven by the MetaMorph software package (version 3.0; Universal Imaging). The exposure times were 1 s for both Oregon green and DAPI (see Fig. 4) and 500 ms for all fluorophores (see Fig. 7).

All images were transferred to a Power Macintosh computer and processed by using Adobe Photoshop version 4.0. Images of control cells were captured and processed identically to those of cells carrying *ponA*-FLAG or *ponA*::Sp$^r$. Cell lengths were determined on images of Oregon green-WGA-stained cells by using the public domain NIH Image program (38a) and by drawing a straight (straight cells) or segmented (bent cells) central line between the two poles of each cell and converting the obtained pixel value to micrometers. A pole was either a free hemispherical cap at the end of a cell or a very bright green band between two cells in a chain. By double staining of cells with propidium iodide and Oregon green-WGA, completed septa were found to stain much brighter with Oregon green-WGA than nascent septa (data not shown). Although a small fraction (<5%) of the completed septa scored may be incomplete septa, the average cell length obtained by this method (3.9 μm; $n = 137$) for wild-type cells grown with a doubling time of 32 min is within the range of those reported for *B. subtilis* SG38 grown with doubling times of 40 min (3.6 μm) and 30 min (4.5 μm), respectively (51).

**Electron microscopy.** Vegetative *B. subtilis* cells grown in 2× YT medium at 37°C were fixed, processed, and analyzed by transmission electron microscopy as described previously (50).

## RESULTS

**Epitope tagging of PBP1.** To localize PBP1 in *B. subtilis* by immunofluorescence microscopy, we added the FLAG epitope (DYKDDDDK) at the C terminus of PBP1. The FLAG epitope is very hydrophilic (pI of 3.85) and hence has a high probability of being surface localized. By using PCR and a plasmid for integration into the *B. subtilis* chromosome by a single crossover event (see Materials and Methods), we generated a strain (LP27) in which a 24-bp sequence encoding the FLAG epitope was inserted into the chromosomal *ponA* gene (45) immediately before the stop codon. Note that this tagged *ponA* (*ponA*-FLAG) is the only *ponA* gene in this strain. To verify the presence of FLAG-tagged PBP1, membranes from log-phase cells of strain LP27 (*ponA*-FLAG) grown at 37°C in 2× YT medium were prepared and membrane proteins were analyzed by SDS–10% PAGE and immunoblotting with a monoclonal anti-FLAG antibody. As shown in Fig. 1A, membranes from *ponA*-FLAG cells (lane 1) contained a protein of about 107 kDa that was recognized by the FLAG antibody while no protein bands were detected in the lanes containing membranes from wild-type cells (strain PS832; lane 3) or cytoplasmic proteins from *ponA*-FLAG cells (lane 2). The calculated molecular mass of PBP1-FLAG is 100.6 kDa, which corresponds roughly to the size of the band detected by immunoblotting. Thus, PBP1-FLAG can be specifically detected in membranes from *ponA*-FLAG cells by using the monoclonal anti-FLAG antibody.

**PBP1-FLAG is functionally indistinguishable from PBP1.** To determine whether PBP1 function is affected by the addition of the FLAG epitope, we first tested whether PBP1-FLAG is able to bind penicillin. Membranes from log-phase cultures of wild-type and *ponA*-FLAG cells grown at 37°C in 2× YT medium were incubated with FLU-C6-APA, proteins separated by SDS–10% PAGE and PBPs visualized on a fluorimager. The results indicated that PBP1-FLAG is capable of binding penicillin like wild-type PBP1 (Fig. 1B), suggesting that tagging with FLAG at the C terminus of PBP1 does not significantly affect the penicillin-binding activity of the protein. Recent experiments conducted in our laboratory have shown that *ponA* mutant cells require increased levels of divalent cations in the growth medium and are therefore unable to grow in Penassay broth, which is relatively low in $Mg^{2+}$ (35). We therefore compared the growth rate of *ponA*-FLAG cells grown in Penassay broth at 37°C to those of wild-type cells and cells of a *ponA* mutant strain (PS2062) lacking PBP1 (45). Consistent with previous findings (35), the *ponA* mutant was unable to grow in Penassay broth, while both the *ponA*-FLAG and wild-type cells grew with a doubling time of about 20 min. In addition, fluorescence microscopy of cells grown at 37°C in 2× YT medium revealed that *ponA*-FLAG cells are morphologically identical to wild-type cells (data not shown, and see below), while *ponA* mutant cells are much longer and thinner (46). These findings indicate that PBP1-FLAG is functionally equivalent to wild-type PBP1 in vivo, and it is therefore very unlikely that the FLAG epitope interferes with PBP1 localization.

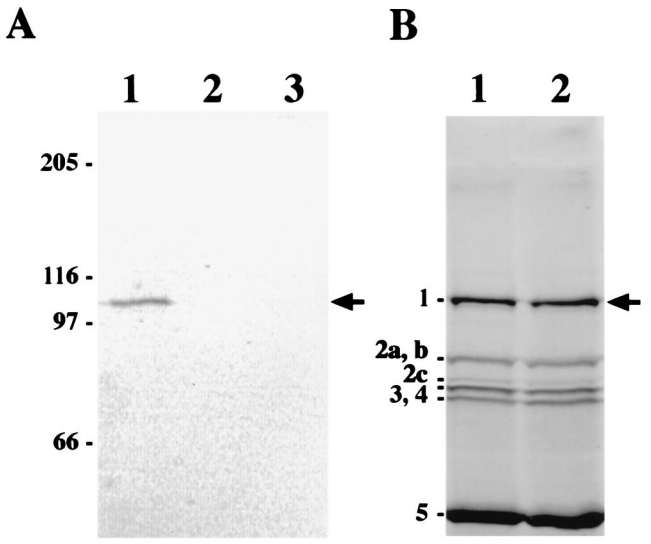


FIG. 1. Immunodetection and penicillin-binding activity of PBP1-FLAG. (A) Western blot of PBP1-FLAG. Membranes from cells grown at 37°C in 100 ml of 2× YT medium were prepared and proteins were solubilized in SDS sample buffer and subjected to SDS–10% PAGE as described in Materials and Methods; about 40 μg of protein was loaded into each well of the gel. The gel was transferred to a polyvinylidene difluoride membrane, which was probed with 4 μg of monoclonal anti-FLAG antibody (Sigma) per ml, and bound antibodies were visualized by using alkaline phosphatase-conjugated secondary antibodies and a colorimetric alkaline phosphatase substrate as described in Materials and Methods. Lanes: 1, membrane proteins from strain LP27 expressing PBP1-FLAG; 2, cytoplasmic proteins from strain LP27; and 3, membrane proteins from wild-type cells (PS832). Molecular mass markers are shown in kilodaltons on the left. The arrow indicates the position of PBP1-FLAG. (B) Penicillin-binding activity of PBP1-FLAG. Membranes were prepared as described for panel A and incubated with FLU-C6-APA for 30 min at 30°C as described (46), proteins (60 μg per well) were separated by SDS–10% PAGE, and PBPs were visualized with a fluorimager. Lanes: 1, membrane proteins from strain LP27 expressing PBP1-FLAG; and 2, membrane proteins from wild-type cells (PS832). The positions of the major vegetative *B. subtilis* PBPs are shown on the left. The arrow indicates the position of PBP1 and PBP1-FLAG (due to the large size of PBP1, we could not observe any size difference between PBP1 and PBP1-FLAG).

**Number of PBP1 molecules per cell.** To date one of the least-abundant bacterial proteins that has been localized by immunofluorescence microscopy is FtsI from *E. coli* (60), which is present at about 100 molecules per cell (13, 60). To determine whether it would be feasible to localize PBP1-FLAG in *B. subtilis* by immunofluorescence microscopy, the cellular abundance of this protein was analyzed. Membranes

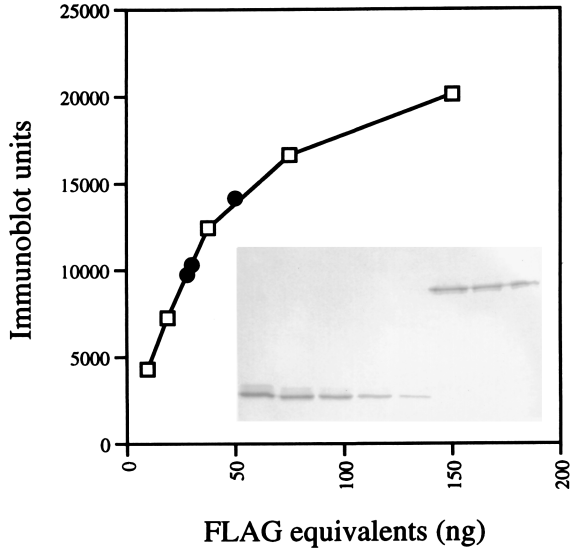


FIG. 2. Quantitative Western blotting of PBP1-FLAG. Cells of strain LP27 were grown in 50 ml of 2× YT medium at 37°C, harvested, and broken by sonication and the membrane and cytoplasmic fractions were separated by high-speed centrifugation as described in Materials and Methods. Membranes were resuspended in 90 μl of buffer B (50 mM Tris-HCl [pH 8], 1 mM β-ME, 1 mM PMSF), and 5, 3, or 2 μl was brought to a 10-μl volume with buffer B, mixed with 10 μl of 2× SDS sample buffer, boiled for 4 min, and subjected to SDS–10% PAGE and immunoblotting with anti-FLAG antibody as described in the legend for Fig. 1A. The blot was scanned, and the relative amounts of FLAG molecules in the samples were determined by comparison with known amounts (range, 9.4 to 150 ng) of purified FLAG-BAP protein (Sigma), which were run on the same gel. The number of PBP1-FLAG molecules per cell was calculated as described in the text. The inset in the graph shows the blot with the different amounts of FLAG-BAP (lower band) and PBP1-FLAG (upper band). Open squares in the graph are values for FLAG-BAP standard protein; black circles are values for the different amounts of membranes from *ponA*-FLAG mutant cells loaded on the gel.

from *ponA*-FLAG cells grown at 30 or 37°C in 2× YT medium were prepared and subjected to SDS–10% PAGE followed by immunoblotting with the anti-FLAG antibody. The blots were scanned, and the total amount of FLAG epitope in each sample was determined by using C-terminal FLAG-BAP as a standard. An example of this analysis is shown in Fig. 2. The DNA content of the samples used for the membrane preparations was determined and used to calculate the amount of PBP1-FLAG molecules per DNA equivalent in the samples. Assuming that FLAG-BAP and PBP1-FLAG react equally well with the anti-FLAG antibody, and by using a molecular weight for the *B. subtilis* chromosome of $2{,}781.77 \times 10^6$ (28) and a molecular weight of FLAG-BAP of 49,100, the numbers of PBP1 molecules per chromosome equivalent were estimated to be $154 \pm 33$ for cells grown at 30°C with a doubling time of 32 min and $231 \pm 86$ for cells grown at 37°C with a doubling time of 20 min (three independent experiments). *B. subtilis* cells grown in media with doubling times of 40 or 30 min contain about 2.9 or 3.3 chromosomes per cell, respectively (51). Hence, we estimate that there are between 450 and 1,000 molecules of PBP1 per cell in our experiments. Using a method based on in vivo labeling of PBPs with [$^3$H]benzylpenicillin, the numbers of molecules of PBP1a and PBP1b per *E. coli* cell have been estimated to be 221 and 127, respectively, for cells grown at 35°C in Luria-Bertani medium (13).

**PBP1 localizes to division sites.** We used log-phase *ponA*-FLAG cells to determine the subcellular localization of PBP1 by immunofluorescence microscopy. Briefly, cells were fixed, permeabilized, applied to poly-L-lysine-coated microscope slides, and incubated with anti-FLAG antibody followed by incubation with biotinylated secondary antibodies and streptavidin conjugated to the red fluorophore Cy3 (Jackson ImmunoResearch). The cells were also stained with WGA conjugated to the fluorophore Oregon green (Molecular Probes) to allow visualization of cell walls and septa. Cells from a log-phase culture of the wild-type strain (PS832) were subjected to the same treatments to serve as a negative control. Fluorescence microscopy of immunostained *ponA*-FLAG cells revealed the presence of bright red bands of fluorescence at division sites (Fig. 3A, B, and C), which were absent in wild-type cells analyzed in parallel (Fig. 3D). We also found no such fluorescent bands in vegetative cells of a strain expressing C-terminal FLAG-tagged GerBA (a putative membrane protein that is normally expressed in the forespore during sporulation and hence has no role in cell division [12]) from a xylose-inducible promoter (39), ruling out the possibility that the targeting of PBP1-FLAG to the division site is due only to the FLAG epitope. About 69% of the *ponA*-FLAG cells examined ($n = 182$) showed *ponA*-FLAG localization at midcell (Fig. 3A, B, and C), while the remaining 31% had no midcell bands. In addition, some fluorescent bands (17% of 151 fluorescent bands observed) were found to colocalize with septa separating two cells in a chain (Fig. 3A, B, and C). Presumably these bands represent PBP1 that was left over from a previous division event. In some cells, the red fluorescence observed was a bright dot rather than a band. Such dots could reflect PBP1 localization or may be a fixation artifact. In numerous experiments we found that if cells are not fixed sufficiently, bright dots could often be observed at old poles, at new poles, and at what appear to be future cell division sites (i.e., at midcell and at one-fourth and three-fourths of the cell's length). Initially we thought that these dots reflected PBP1 localization, and it has become apparent to us that extreme caution must be taken when interpreting data from such immunofluorescence experiments. In general, we found that cells that are not properly fixed have a high background fluorescence and look very smudgy compared with cells that are properly fixed. Other authors have previously reported that the presence of dots at the cell pole is a common artifact associated with immunofluorescence microscopy of bacteria (60). Taken together, the results suggest that PBP1 localizes to midcell around the time that the cell is about to divide and disappears from this site shortly after completion of the septum.

**Impaired septum formation in a mutant lacking PBP1.** The evidence that PBP1 is localized predominantly to the site of cell division suggests that this protein might have some important role in septum formation, and recent results acquired in our laboratory suggest that PBP1 is required for septum formation in cells grown in media low in $Mg^{2+}$ (35). It has previously been shown that in 2× SG medium, *ponA* mutant cells are longer and grow more slowly than wild-type cells; in 2× YT and minimal medium, growth of *ponA* mutant cells is also significantly slower than that of wild-type cells (46). Given that PBP1 localizes to division sites in cells grown in 2× YT medium, we speculated that PBP1 may also be needed for septum formation under these normal growth conditions. Indeed, fluorescence microscopy of *ponA* mutant cells grown in 2× YT medium at 30°C and double stained with Oregon green-WGA and DAPI to visualize cell walls, septa, and nucleoids showed that *ponA* mutant cells not only are longer than wild-type cells (mean cell length was 6.4 μm for *ponA* mutant cells [$n = 98$] and 3.9 μm for wild-type cells [$n = 137$]), consistent with a previous report (46), but also contain a larger average number of nucleoids per cell (2.5; $n = 98$) than wild-type cells (1.8; $n =$

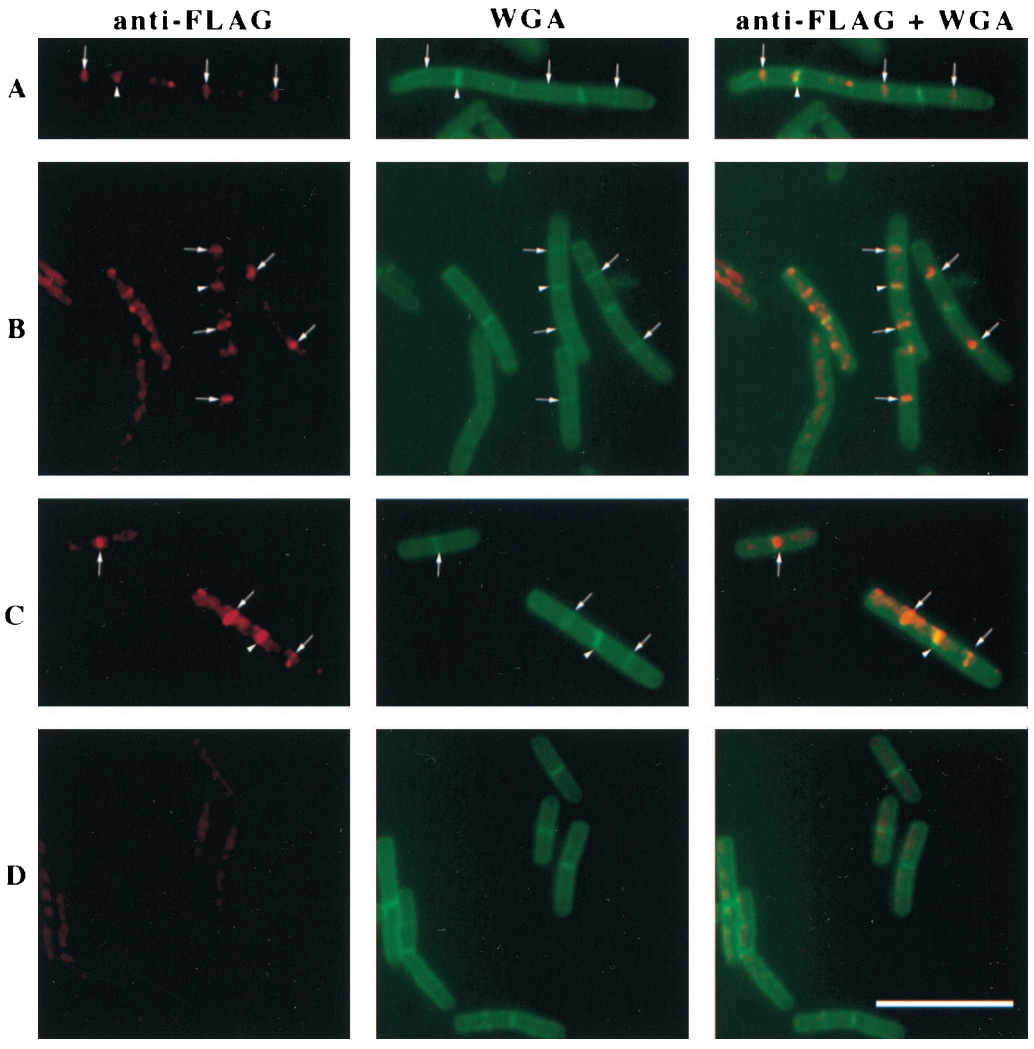


FIG. 3. Immunofluorescence of *ponA*-FLAG (A, B, and C) or wild-type (D) cells grown in 2× YT medium at 37°C. The figure shows immunodetection of the FLAG epitope only (red), staining of cell walls and septa with Oregon green-conjugated WGA (green), and an overlay of those images showing simultaneously visualized PBP1-FLAG and cell walls and septa. Arrows point to PBP1-FLAG localization at midcell; arrowheads show PBP1-FLAG bands that colocalize with completed septa between two cells in a chain (completed septa stain very brightly with Oregon green-WGA, in contrast to nascent septa at midcell, which appear as faint green bands; see also Materials and Methods). Bar, 10 μm.

137), suggesting a reduced efficiency of septation of the *ponA* mutant (Fig. 4 and 5). Similar results were obtained when cells were grown at 37°C (results not shown). Interestingly, bright green dots could often be observed at the periphery of Oregon green-WGA-stained *ponA* mutant cells grown in 2× YT medium at 30°C (39% of the cells; $n = 163$) (Fig. 4A) or at 37°C (39%; $n = 222$), suggesting that at these sites septation was initiated but failed to go to completion. The proportion of *ponA* mutant cells with bright green dots was lower, but still significant, when the cells were grown in 2× YT medium to which 1 mM or 10 mM $MgCl_2$ had been added (23% of the cells [$n = 279$] grown at 37°C in 2× YT with 1 mM $MgCl_2$ had bright green dots, while with 10 mM $MgCl_2$, the number was 25% [$n = 282$]), suggesting that the lack of PBP1 results in a significant septation defect even under these conditions. Based on electron microscopy data (Fig. 6, and see below) we estimate that about 50% of the cell wall dots were located between well-segregated nucleoids while the remaining dots were located at positions overlapping the DNA. No cell wall dots were observed in wild-type cells ($n = 339$) grown at 37°C in 2× YT medium, indicating that the observed septation defect was indeed due to the *ponA* mutation.

To investigate the septation defect of the *ponA* mutant in more detail, sections of *ponA* mutant and wild-type cells were prepared and examined by electron microscopy (Fig. 6). This analysis showed that while most dividing *ponA* mutant cells (73%; $n = 103$) had septa that looked like those of wild-type cells (Fig. 6C), a significant proportion (27%; $n = 103$) had abnormal clusters of cell wall material assembled at distinct sites at the cell periphery (Fig. 6A) or displayed incomplete septa with aberrant morphology (Fig. 6B). Presumably these abnormal septa or wall clusters correspond to the fluorescent dots seen by fluorescence microscopy of *ponA* mutant cells (Fig. 4A, and see above), and this observation further supports a role for PBP1 in septal peptidoglycan synthesis. However, it cannot be ruled out that these abnormal septa or cell wall clusters are a secondary effect of the reduced diameter and/or general changes in the cell wall structure of the *ponA* mutant (46).

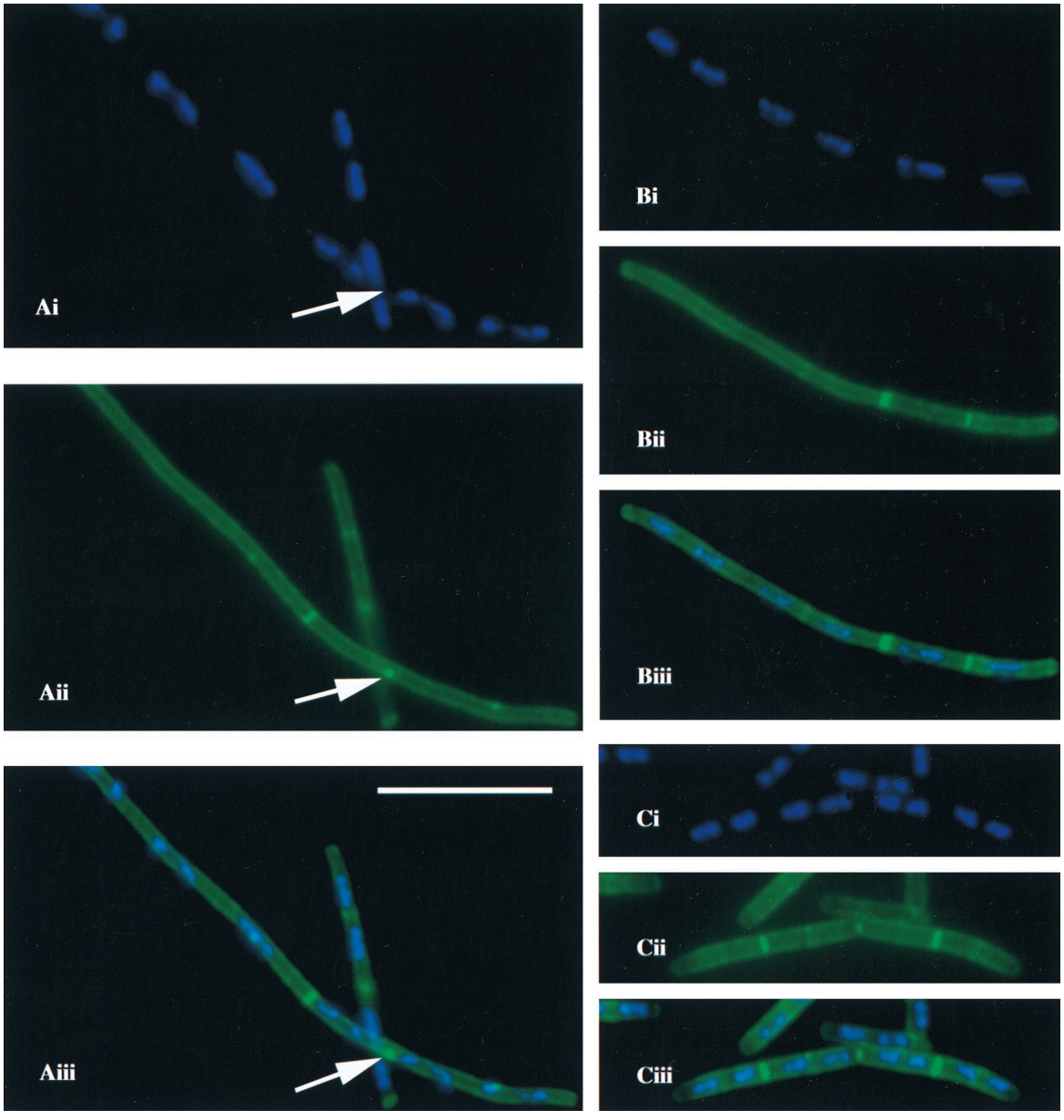


FIG. 4. Fluorescence micrographs showing filamentation in a *ponA* mutant (strain PS2062) grown at 30°C in 2× YT medium. (A and B) *ponA* mutant cells; (C) wild-type cells. (Ai, Bi, and Ci) DAPI staining of nucleoids (blue); (Aii, Bii, and Cii) staining of cell walls and septa with Oregon green-conjugated WGA (green); (Aiii, Biii, and Ciii) overlay of DAPI staining and cell wall staining. Bar, 10 μm. Arrows in panels Aii and Aiii show a bright green dot in the periphery of *ponA* mutant cells between two nucleoids (arrow in Ai). Such dots were seen in 39% of the *ponA* mutant cells examined ($n = 163$) but were not seen in wild-type cells (0%; $n = 137$). Similar results were obtained when cells were grown in 2× YT medium at 37°C (39% of the *ponA* mutant cells had dots [$n = 222$]; 0% of wild-type cells had dots [$n = 339$]).

**FtsZ localization in cells lacking PBP1.** An essential and very early event in cell division is the assembly and polymerization of FtsZ into a cytokinetic ring at midcell (9, 48). Given the effect of the *ponA* mutation on septum formation, we were interested in analyzing the effect of this mutation on FtsZ ring formation. Log-phase cultures of *ponA* mutant and wild-type cells were fixed and subjected to immunofluorescence microscopy by using a rabbit antiserum against *B. subtilis* FtsZ followed by staining with Cy3-conjugated secondary antibodies as well as DAPI and FITC-conjugated WGA to visualize nucleoids, septa, and cell walls. Examination of the immunostained cells showed that the *ponA* mutation had a significant but very pleiotropic effect on FtsZ localization. Some *ponA* mutant cells had normal FtsZ localization, which was seen as a bright ring-like structure at the midpoint of the cell with one or two well-segregated nucleoids on each side (Fig. 7B, leftmost cell). Others had two closely positioned FtsZ rings at anticipated division sites, which were not always perpendicular to the long axis of the cell (Fig. 7A). Cells with normal-appearing FtsZ rings at inappropriate sites, such as an acentric ring in a cell with three or more nucleoids (Fig. 7B), as well as cells with no visible FtsZ rings, were also observed. In some of the latter cells, a diffuse or fuzzy signal between two separated nucleoids was sometimes detected, suggestive of aggregated or disassem-

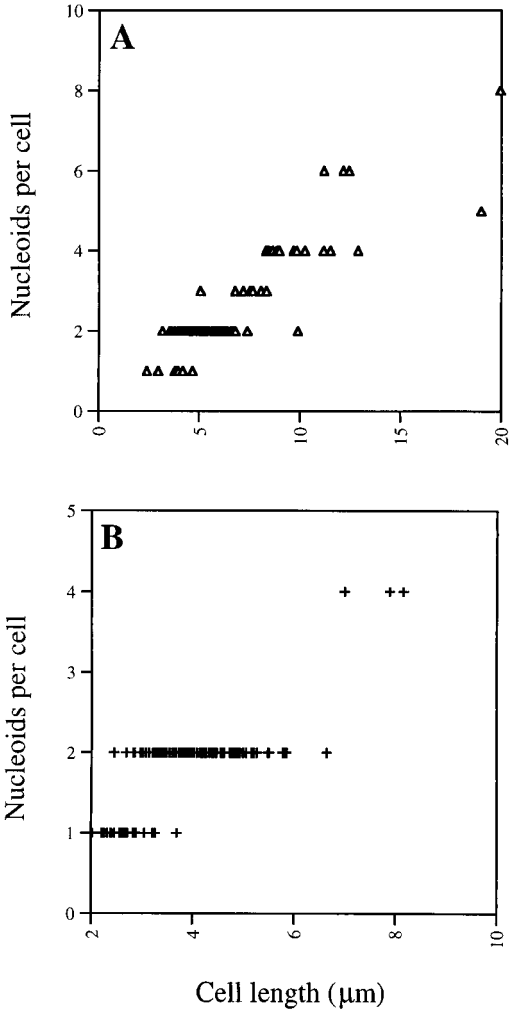


FIG. 5. Cell length and number of nucleoids for *ponA* mutant (A) and wild-type (B) cells grown at 30°C in 2× YT medium. Images similar to those shown in Fig. 4 were used for the analysis. Cell lengths were measured as described in Materials and Methods, and the number of visible, fully segregated nucleoids present in each cell was counted. A total of 98 and 137 cells are depicted in panels A and B, respectively. The mean cell length and nucleoid content obtained were, respectively, 6.4 μm and 2.5 for *ponA* mutant cells and 3.9 μm and 1.8 for wild-type cells.

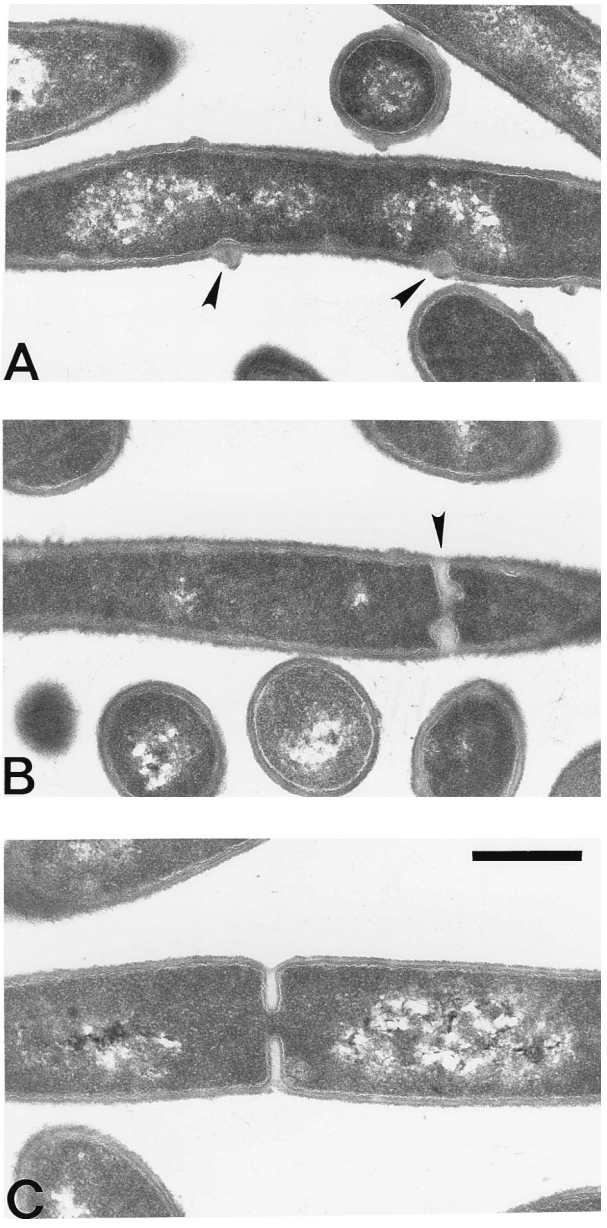


FIG. 6. Electron micrograph showing cross-sections of *ponA* mutant and wild-type cells grown at 37°C in 2× YT medium. (A and B) *ponA* mutant cells; (C) wild-type cell. The arrowheads indicate aberrant septa or cell wall clusters in *ponA* mutant cells. Note that the cell wall clusters shown in panel A are at positions overlapping the DNA. Bar, 0.5 μm.

bled FtsZ protein. To compare FtsZ localization in *ponA* mutant and wild-type cells, immunostained cells were scored for FtsZ localization by using the following criteria: (i) normal FtsZ rings, which were defined as a nice ring-like localization at the midpoint of the cell with one or two separated nucleoids on each side; (ii) abnormal FtsZ rings, which were either double rings or FtsZ rings at inappropriate sites; and (iii) no FtsZ rings, a category used when cells had one or two nucleoids and no FtsZ rings. This analysis showed that most *ponA* mutant cells (52%; $n = 507$) had normal FtsZ rings and a significant proportion (22%; $n = 507$) had abnormal FtsZ rings, while the remaining 26% ($n = 507$) had no FtsZ rings. In contrast, 82% ($n = 425$) of the wild-type cells had normal FtsZ rings and 3% ($n = 425$) had abnormal rings, while 15% ($n = 425$) showed no FtsZ rings (Table 2). These results therefore demonstrate that the *ponA* mutation has a significant, but very pleiotropic, effect on FtsZ localization, presumably because the effects of the *ponA* mutation itself are very pleiotropic (35, 46).

## DISCUSSION

The main contributions of the present work can be summarized as follows: (i) PBP1 localizes to the division site in *B. subtilis* cells, (ii) a significant proportion of *ponA* mutant cells grown under normal growth conditions are filamentous or have a septation defect, and (iii) while FtsZ localizes correctly in most *ponA* mutant cells grown under normal conditions, a significant proportion of *ponA* mutant cells contain FtsZ rings that have aberrant morphology or are localized at inappropriate sites.

**Role of PBP1 in septum formation.** The localization of PBP1 to the division site strongly suggests that PBP1 is directly involved in septal peptidoglycan synthesis. The only other PBP

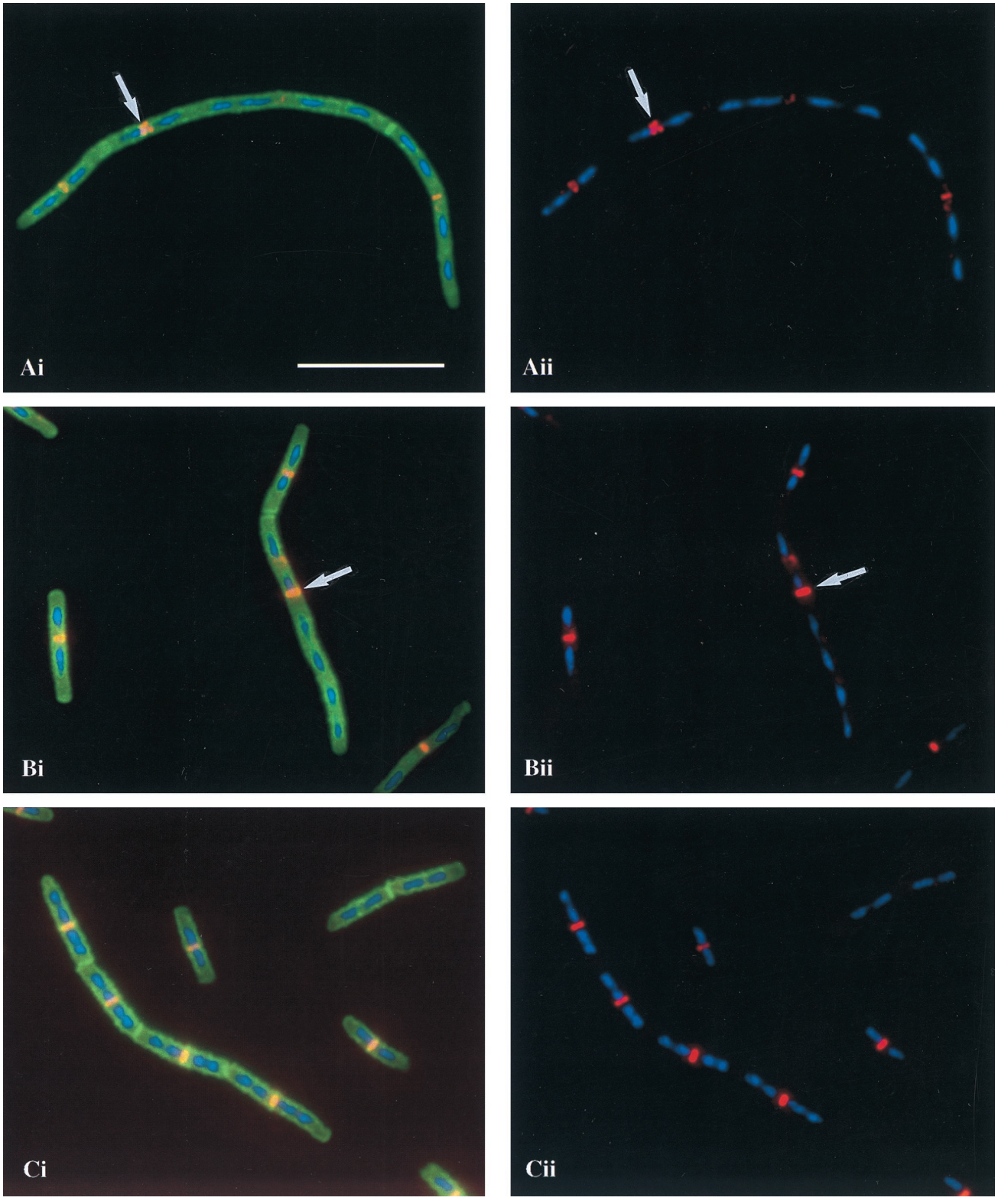


FIG. 7. Immunolocalization of FtsZ in *ponA* mutant (A and B) and wild-type (C) cells grown in 2× YT medium at 37°C. (Ai, Bi, and Ci) Overlay of FtsZ localization (red and yellow), DAPI staining of nucleoids (blue), and staining of cell walls and septa with FITC-conjugated WGA (green); (Aii, Bii, and Cii) overlay of FtsZ localization (red) and DAPI staining (blue). The arrows in panels Ai and Aii indicate an aberrant FtsZ ring, and those in panels Bi and Bii indicate an FtsZ ring at an inappropriate location. Bar, 10 μm.

TABLE 2. FtsZ localization patterns

| FtsZ pattern[a] | Number (%) of cells of[b]: | |
|---|---|---|
| | Wild-type strain | *ponA* mutant strain |
| Normal | 348 (82) | 262 (52) |
| Abnormal | 11 (3) | 112 (22) |
| No rings | 66 (15) | 33 (26) |

[a] Normal is a single FtsZ ring at midcell with one or two separate nucleoids on both sides, abnormal is double rings, fuzzy or diffuse localization, or rings at inappropriate locations, such as an acentric ring in a cell with three or more nucleoids, and no rings is a cell with one or two nucleoids and no FtsZ ring.
[b] Cells in fields like those shown in Fig. 7 were used for the analysis.

that has been directly implicated in septum synthesis is the class B HMW PBP2b, which is homologous to *E. coli* FtsI (62). Given that class B HMW PBPs have no transglycosylase activity (1, 17, 57), it is likely that PBP2b and PBP1 cooperate during septal peptidoglycan synthesis in *B. subtilis*, as has been proposed for *E. coli* FtsI and PBP1a and PBP1b (61). However, in contrast to PBP2b, which is an essential protein (62), inactivation of *ponA* is not lethal under normal growth conditions (35, 45, 46). This suggests the presence in *B. subtilis* of another protein with transglycosylase activity involved in septum synthesis. Possible candidates for such a protein are the two other known *B. subtilis* HMW class A PBPs, PBP2c and PBP4, because previous studies have shown that the growth and morphology defects associated with a *ponA* insertional mutation are exacerbated greatly by the additional loss of PBP4 and only slightly by the loss of PBP2c (46). However, cells lacking PBP4, PBP2c, or both do not display any significant growth defects under normal growth conditions (43, 44, 46), suggesting that any contribution of either of these proteins to septal wall synthesis is clearly dispensable when PBP1 is present. Furthermore, a mutant lacking the PBPs PBP1, PBP2c, and PBP4 is viable, although its growth is seriously impaired (46), suggesting the involvement of yet another (unknown) protein. Recently the *B. subtilis* genome sequencing project identified *ywhE* as a gene encoding a putative class A HMW PBP (28). We are now planning to generate a mutant that lacks all four class A HMW PBP-encoding genes to determine whether such a mutant is viable. In this respect it is worth noting that inactivation of PBP1a and PBP1b in *E. coli* is lethal (63), despite the presence of a third class A HMW PBP in this organism (23) as well as a putative monofunctional peptidoglycan transglycosylase (54). Inactivation of a single *ponA* homolog in *Neisseria gonorrhoeae* is also lethal (47), again despite the presence of a putative monofunctional peptidoglycan transglycosylase in this organism (54).

**Septal peptidoglycan synthesis is not the only function of PBP1.** Previous studies have shown that inactivation of *ponA* produces cells that are not only longer than wild-type cells but also thinner and more bent (46), suggesting a role for PBP1 in lateral wall synthesis. In contrast, *B. subtilis* cells containing a C-terminal truncated version of PBP2b, a protein presumed to function only in cell division, grow as filaments, but their cell diameter was not significantly different from that of wild-type cells (62). In addition, our results do not exclude the possibility that PBP1 is present in the membrane lining the cylindrical parts of the cell wall, because the local concentration of PBP1 at such sites may be too low to be detected. Taken together, the results make it seem likely that during cell elongation, PBP1 is involved in cylindrical cell wall synthesis and is present at fairly low local concentrations at a number of sites in the membrane lining the cylinder. Subsequently, upon initiation of cell division, PBP1 localizes to the midpoint of the cell by some unknown mechanism, becomes part of the divisome complex (37), and promotes the formation of septal peptidoglycan, possibly by synthesizing primers which are subsequently crosslinked by PBP2b.

**Timing of PBP1 localization.** One of the earliest events in septation in *E. coli* is the polymerization of the tubulin-like FtsZ protein into a cytokinetic ring at midcell, which contracts during the septation process and maintains a position at the leading edge of the invaginating septum (9, 48). Formation of the FtsZ ring occurs in the absence of functional FtsA, FtsQ, FtsI, FtsK, or FtsW (2, 4, 27, 64). Conversely, septal localization of FtsA and FtsK is FtsZ-dependent (4, 64) and FtsI localization depends on FtsZ, FtsA, FtsL, and FtsQ (58, 59), while FtsN localization depends on prior FtsZ and FtsA localization and requires the function of FtsI and FtsQ (3). In most cases, these localization studies are indicative of the stage in septation during which a given protein acts. For example, *ftsZ* mutant cell filaments have a smooth morphology, indicating a role for FtsZ very early in the division process (8, 56), while *ftsI* mutant cell filaments have indentations at septal positions suggesting a role for FtsI in the continuation rather than initiation of septum formation (36, 38). Inactivation of PBP1a and PBP1b with the antibiotics cefsulodin and moenomycin, which inhibit the transpeptidase activity and transglycosylase activity, respectively, does not prevent initiation of constriction during cell division in *E. coli* (36, 61), suggesting that PBP1a and PBP1b, like FtsI, are not required for initiation of septum formation in *E. coli*.

In the present study we found that 17% of 151 fluorescent PBP1 bands observed colocalized with completed septa between two cells in a chain (Fig. 3A, B, and C). In addition, in the majority of cells with midcell PBP1 fluorescence (70% of 126 cells), septal peptidoglycan was also visible at these positions as judged by the presence of faint green bands upon staining with Oregon green-WGA. This is in contrast to FtsZ, which was not observed to colocalize with septa visualized by FITC-WGA staining (Fig. 7 and data not shown), suggesting that PBP1 localizes to the division site after assembly of the FtsZ ring and that PBP1 probably acts at a relatively late stage in septation. In support of this idea, immunofluorescence and electron microscopy of *B. subtilis ponA* mutant cells showed that a significant proportion of the cells (27 to 39%) had abnormal septa or clusters of cell wall material at the cell periphery, indicating that in such cells, septum formation had initiated but failed to complete. Furthermore, by immunofluorescence microscopy of *ponA* mutant cells we found that FtsZ rings formed normally in the majority of the cells (56%; $n = 507$), indicating that localization of FtsZ to the division site does not require prior localization of PBP1. However, we also found that a significant proportion of the *ponA* mutant cells (22%; $n = 507$) contained FtsZ rings that had aberrant morphology or were present at inappropriate locations, indicating that the lack of PBP1 somehow interferes with the stability or assembly of the FtsZ ring. That the effect of the *ponA* mutation on FtsZ localization is so pleiotropic is not surprising, given that PBP1 is involved not just in cell division but also in lateral cell wall synthesis and maintenance of the correct cell diameter, as discussed above. Consequently, we find it difficult to explain precisely how the *ponA* mutation affects FtsZ localization, but there are several possibilities: (i) the reduction of the diameter of the cell could affect FtsZ ring assembly or stability; (ii) some general change in the cell wall structure may alter interactions between the cell wall and the membrane, which in turn may interfere with the binding of FtsZ to its membrane nucleation site; (iii) changes in septal peptidoglycan structure

or interactions between proteins at the division site could interfere with the stability of the FtsZ ring; and (iv) effects on cell growth might interfere with general cues for cell division. However, we think it is important to stress that the majority of the *ponA* mutant cells had normal FtsZ localization, indicating that PBP1 is not completely essential for the localization and binding of FtsZ at the division site.

Interestingly, some of the FtsZ localization patterns observed in the *ponA* mutant are reminiscent of those reported in a study by Addinall and colleagues (2) for *E. coli* filaments with mutations in the *ftsA*, *ftsQ*, or *ftsI* gene. These authors found that a large proportion of such filaments had more than two FtsZ rings, some had indentations or FtsZ rings with variable spacing, and some filaments had no FtsZ rings, and they suggested that blocking of septal peptidoglycan synthesis blocks progression of the FtsZ ring and may thus lead to its destabilization (2). In a similar study it was found that inactivation of FtsI by temperature or cephalexin also had very pleiotropic effects on FtsZ localization, and it was shown that inactivation of FtsI inhibits constriction of the FtsZ ring and delays the assembly of FtsZ rings at future division sites, resulting in a lower overall average number of FtsZ rings per cell under these conditions (40). It is possible that the lack of PBP1 at the septum in *B. subtilis* affects FtsZ ring formation by a similar mechanism.

Recently it was shown by fluorescence microscopy that *E. coli* cells which lack a protein required for the synthesis of the major membrane lipid component phosphatidylethanolamine (PE) have a defect in cell division and contain FtsZ rings with aberrant structure at potential division sites (reference 33 and references therein). For example, some PE-deficient filaments were found to contain FtsZ bands that were not perpendicular to the long axis of the cell, a number of very long filaments only had a few FtsZ rings, and others had regularly spaced FtsZ rings with normal morphology (33). One suggested explanation for these findings is that changes in the phospholipid composition of the cell membrane may affect FtsZ ring formation indirectly by altering the interaction between FtsZ and its membrane nucleation site (33). Given the effect of the *ponA* mutation on overall cell wall structure and cell dimensions, the cell membrane structure may also be affected and consequently the inactivation of *ponA* may affect FtsZ ring formation by a mechanism similar to that of PE deficiency.

## ACKNOWLEDGMENTS

We thank David L. Popham for the gift of plasmid pDPC273 and for advice regarding epitope tagging of PBP1, Petra A. Levin for the gift of anti-FtsZ antibodies and for helpful discussions, Kit Pogliano and Ann Cowan for helpful advice regarding immunofluorescence microscopy, Arthur L. Hand for performing electron microscopy, Frank Morgan and Susan Krueger for assistance with computer work and image analysis, Richard Losick for generous support and use of his equipment, Madan Paidhungat for the $P_{xyl}$-GerBA-FLAG strain, and Lawrence I. Rothfield for helpful discussions and comments on the manuscript.

This work was supported by a grant from the National Institutes of Health to P.S. (GM19698), a postdoctoral fellowship from the Danish Natural Science Research Council to L.B.P. (9601026), and a postdoctoral fellowship to E.R.A. from the Jane Coffin Childs Memorial Fund for Medical Research.

## REFERENCES

1. **Adam, M., C. Fraipont, N. Rhazi, M. Nguyen-Distèche, B. Lakaye, J.-M. Frère, B. Devreese, J. van Beeumen, Y. van Heijenoort, J. van Heijenoort, and J.-M. Ghuysen.** 1997. The bimodular G57-V577 polypeptide chain of the class B penicillin-binding protein 3 of *Escherichia coli* catalyzes peptide bond formation from thiolesters and does not catalyze glycan chain polymerization from the lipid II intermediate. J. Bacteriol. **179:**6005–6009.
2. **Addinall, S. G., E. Bi, and J. Lutkenhaus.** 1996. FtsZ ring formation in *fts* mutants. J. Bacteriol. **178:**3877–3884.
3. **Addinall, S. G., C. Cao, and J. Lutkenhaus.** 1997. FtsN, a late recruitment to the septum in *Escherichia coli*. Mol. Microbiol. **25:**303–309.
4. **Addinall, S. G., and J. Lutkenhaus.** 1996. FtsA is localized to the septum in an FtsZ-dependent manner. J. Bacteriol. **178:**7167–7172.
5. **Allen, K. A., A. Neuberger, and N. Sharon.** 1973. The purification, composition and specificity of wheat-germ agglutinin. Biochem. J. **131:**155–162.
6. **Anagnostopoulus, C., and J. Spizizen.** 1961. Requirements for transformation in *Bacillus subtilis*. J. Bacteriol. **81:**74–76.
7. **Bayer, M. H., W. Keck, and M. E. Bayer.** 1990. Localization of penicillin-binding protein 1b in *Escherichia coli*: immunoelectron microscopy and immunotransfer studies. J. Bacteriol. **172:**125–135.
8. **Begg, K. J., and W. D. Donachie.** 1985. Cell shape and division in *Escherichia coli*: experiments with shape and division mutants. J. Bacteriol. **163:**615–622.
9. **Bi, E., and J. Lutkenhaus.** 1991. FtsZ ring structure associated with division in *Escherichia coli*. Nature **354:**161–164.
10. **Bramhill, D.** 1997. Bacterial cell division. Annu. Rev. Cell Dev. Biol. **13:** 395–424.
11. **Chen, J. C., D. S. Weiss, J.-M. Ghigo, and J. Beckwith.** 1999. Septal localization of FtsQ, an essential cell division protein in *Escherichia coli*. J. Bacteriol. **181:**521–530.
12. **Corfe, B. M., A. Moir, D. Popham, and P. Setlow.** 1994. Analysis of the expression and regulation of the *gerB* spore germination operon of *Bacillus subtilis* 168. Microbiology **140:**3079–3083.
13. **Dougherty, T. J., K. Kennedy, R. E. Kessler, and M. J. Pucci.** 1996. Direct quantitation of the number of individual penicillin-binding proteins per cell in *Escherichia coli*. J. Bacteriol. **178:**6110–6115.
14. **Ferrari, F. A., A. Nguyen, D. Lang, and J. A. Hoch.** 1983. Construction and properties of an integrable plasmid for *Bacillus subtilis*. J. Bacteriol. **154:** 1513–1515.
15. **García del Portillo, F., M. A. de Pedro, and J. A. Ayala.** 1991. Identification of a new mutation in *Escherichia coli* that suppresses a *pbpB* (Ts) phenotype in the presence of penicillin-binding protein 1B. FEMS Microbiol. Lett. **84:**7–14.
16. **García del Portillo, F., M. A. de Pedro, D. Joseleau-Petit, and R. d'Dari.** 1989. Lytic response of *Escherichia coli* cells to inhibitors of penicillin-binding proteins 1a and 1b as a timed event related to cell division. J. Bacteriol. **171:**4217–4221.
17. **Ghuysen, J.-M.** 1994. Molecular structures of penicillin-binding proteins and β-lactamases. Trends Microbiol. **2:**372–380.
18. **Goffin, C., C. Fraipont, J. Ayala, M. Terrak, M. Nguyen-Distèche, and J.-M. Ghuysen.** 1996. The non-penicillin-binding module of the tripartite penicillin-binding protein 3 of *Escherichia coli* is required for the folding and/or stability of the penicillin-binding module and the membrane-anchoring module confers cell septation activity on the folded structure. J. Bacteriol. **178:** 5402–5409.
19. **Hale, C. A., and P. A. J. de Boer.** 1997. Direct binding of FtsZ to ZipA, an essential component of the septal ring structure that mediates cell division in *E. coli*. Cell **88:**175–185.
20. **Harry, E. J., K. Pogliano, and R. Losick.** 1995. Use of immunofluorescence to visualize cell-specific gene expression during sporulation in *Bacillus subtilis*. J. Bacteriol. **177:**3386–3393.
21. **Harry, E. J., and R. G. Wake.** 1997. The membrane-bound cell division protein DivIB is localized to the division site in *Bacillus subtilis*. Mol. Microbiol. **25:**275–283.
22. **Hiraga, S., C. Inchinose, H. Niki, and M. Yamazoe.** 1998. Cell cycle-dependent duplication and bidirectional migration of SeqA-associated DNA-protein complexes in *E. coli*. Mol. Cell **1:**381–387.
23. **Höltje, J.-V.** 1998. Growth of the stress-bearing and shape-maintaining murein sacculus of *Escherichia coli*. Microbiol. Mol. Biol. Rev. **62:**181–203.
24. **Ishino, F., K. Mitsui, S. Tamaki, and M. Matsuhashi.** 1980. Dual enzyme activities of cell wall peptidoglycan synthesis, peptidoglycan transglycosylase and penicillin-sensitive transpeptidase, in purified preparations of *Escherichia coli* penicillin-binding protein 1A. Biochem. Biophys. Res. Commun. **97:**287–293.
25. **Katis, V. L., E. J. Harry, and R. G. Wake.** 1997. The *Bacillus subtilis* division protein DivIC is a highly abundant membrane-bound protein that localizes to the division site. Mol. Microbiol. **26:**1047–1055.
26. **Kato, J., H. Suzuki, and Y. Hirota.** 1985. Dispensability of either penicillin-binding protein-1a or -1b involved in the essential process for cell elongation in *Escherichia coli*. Mol. Gen. Genet. **200:**272–277.
27. **Khattar, M. M., S. G. Addinall, K. H. Stedul, D. S. Boyle, J. Lutkenhaus, and W. D. Donachie.** 1997. Two polypeptide products of the *Escherichia coli* cell division gene *ftsW* and a possible role for FtsW in FtsZ function. J. Bacteriol. **179:**784–793.
28. **Kunst, F., N. Ogasawara, I. Moszer, A. M. Albertini, G. Alloni, et al.** 1997. The complete genome sequence of the gram-positive bacterium *Bacillus subtilis*. Nature **390:**249–256.
29. **Laemmli, U. K.** 1970. Cleavage of structural proteins during the assembly of the head of bacteriophage T4. Nature **227:**680–685.
30. **Leighton, T. J., and R. H. Doi.** 1971. The stability of messenger ribonucleic

acid during sporulation in *Bacillus subtilis*. J. Biol. Chem. **254:**3189–3195.
31. **Levin, P. A., and R. Losick.** 1996. Transcription factor Spo0A switches the localization of the cell division protein FtsZ from a medial to a bipolar pattern in *Bacillus subtilis*. Genes Dev. **10:**478–488.
32. **Lowry, O. H., N. J. Rosebrough, A. L. Farr, and R. J. Randall.** 1951. Protein measurement with the Folin phenol reagent. J. Biol. Chem. **193:**265–275.
33. **Mileykovskaya, E., Q. Sun, W. Margolin, and W. Dowhan.** 1998. Localization and function of early cell division proteins in filamentous *Escherichia coli* cells lacking phosphatidylethanolamine. J. Bacteriol. **180:**4252–4257.
34. **Murray, T., D. L. Popham, and P. Setlow.** 1997. Identification and characterization of *pbpA* encoding *Bacillus subtilis* penicillin-binding protein 2A. J. Bacteriol. **179:**3021–3029.
35. **Murray, T., D. L. Popham, and P. Setlow.** 1998. *Bacillus subtilis* cells lacking penicillin-binding protein 1 require increased levels of divalent cations for growth. J. Bacteriol. **180:**4555–4563.
36. **Nanninga, N.** 1991. Cell division and peptidoglycan assembly in *Escherichia coli*. Mol. Microbiol. **5:**791–795.
37. **Nanninga, N.** 1998. Morphogenesis of *Escherichia coli*. Microbiol. Mol. Biol. Rev. **62:**110–129.
38. **Nguyen-Distèche, M., C. Fraipont, N. Buddelmeijer, and N. Nanninga.** 1998. The structure and function of *Escherichia coli* penicillin-binding protein 3. Cell. Mol. Life Sci. **54:**309–316.
38a. NIH Image program. National Institutes of Health, Bethesda, Md. http://rsb.info.gov/nih-image. [9 September 1998, last date accessed.]
39. **Paidhungat, M., L. B. Pedersen, and P. Setlow.** 1999. Unpublished results.
40. **Pogliano, J., K. Pogliano, D. S. Weiss, R. Losick, and J. Beckwith.** 1997. Inactivation of FtsI inhibits constriction of the FtsZ cytokinetic ring and delays the assembly of FtsZ rings at potential division sites. Proc. Natl. Acad. Sci. USA **94:**559–564.
41. **Pogliano, K., E. Harry, and R. Losick.** 1995. Visualization of the subcellular location of sporulation proteins in *Bacillus subtilis* using immunofluorescence microscopy. Mol. Microbiol. **18:**459–470.
42. **Pogliano, K., A. E. M. Hofmeister, and R. Losick.** 1997. Disappearance of the $\sigma^E$ transcription factor from the forespore and the SpoIIE phosphatase from the mother cell contributes to establishment of cell-specific gene expression during sporulation in *Bacillus subtilis*. J. Bacteriol. **179:**3331–3341.
43. **Popham, D. L., and P. Setlow.** 1993. Cloning, nucleotide sequence, and regulation of the *Bacillus subtilis pbpF* gene, which codes for a putative class A high-molecular-weight penicillin-binding protein. J. Bacteriol. **175:**4870–4876.
44. **Popham, D. L., and P. Setlow.** 1994. Cloning, nucleotide sequence, mutagenesis, and mapping of the *Bacillus subtilis pbpD* gene, which codes for penicillin-binding protein 4. J. Bacteriol. **176:**7197–7205.
45. **Popham, D. L., and P. Setlow.** 1995. Cloning, nucleotide sequence, and mutagenesis of the *Bacillus subtilis ponA* operon, which codes for penicillin-binding protein (PBP) 1 and a PBP-related factor. J. Bacteriol. **177:**326–335.
46. **Popham, D. L., and P. Setlow.** 1996. Phenotypes of *Bacillus subtilis* mutants lacking multiple class A high-molecular-weight penicillin-binding proteins. J. Bacteriol. **178:**2079–2085.
47. **Ropp, P. A., and R. A. Nicholas.** 1997. Cloning and characterization of the *ponA* gene encoding penicillin-binding protein 1 from *Neisseria gonorrhoeae* and *Neisseria meningitidis*. J. Bacteriol. **179:**2783–2787.
48. **Rothfield, L. I., and S. S. Justice.** 1997. Bacterial cell division: the cycle of the ring. Cell **88:**581–584.
49. **Sarkar, G., and S. S. Sommer.** 1990. The "megaprimer" method of site-directed mutagenesis. BioTechniques **8:**404–407.
50. **Setlow, B., A. R. Hand, and P. Setlow.** 1991. Synthesis of a *Bacillus subtilis* small, acid-soluble spore protein in *Escherichia coli* causes cell DNA to assume some characteristics of spore DNA. J. Bacteriol. **173:**1642–1653.
51. **Sharpe, M. E., P. M. Hauser, R. G. Sharpe, and J. Errington.** 1998. *Bacillus subtilis* cell cycle as studied by fluorescence microscopy: constancy of cell length at initiation of DNA replication and evidence for active nucleoid partitioning. J. Bacteriol. **180:**547–555.
52. **Sizemore, R. K., J. J. Caldwell, and A. S. Kendrick.** 1990. Alternate gram staining technique using a fluorescent lectin. Appl. Environ. Microbiol. **56:**2245–2247.
53. **Spratt, B. G., and A. B. Pardee.** 1975. Penicillin-binding proteins and cell shape in *E. coli*. Nature **254:**516–517.
54. **Spratt, B. G., J. Zhou, M. Taylor, and M. J. Merrick.** 1996. Monofunctional biosynthetic peptidoglycan transglycosylases. Mol. Microbiol. **19:**639–647.
55. **Suzuki, H., Y. van Heijenoort, T. Tamura, J. Mizoguchi, Y. Hirota, and J. van Heijenoort.** 1980. In vitro peptidoglycan polymerization catalyzed by penicillin binding protein 1b of *Escherichia coli* K12. FEBS Lett. **110:**245–249.
56. **Taschner, P. E. M., P. G. Huls, E. Pas, and C. L. Woldringh.** 1988. Division behavior and shape changes in isogenic *ftsZ*, *ftsQ*, *ftsA*, *pbpB*, and *ftsE* cell division mutants of *Escherichia coli* during temperature shift experiments. J. Bacteriol. **170:**1533–1540.
57. **van Heijenoort, Y., M. Gómez, M. Derrien, J. Ayala, and J. van Heijenoort.** 1992. Membrane intermediates in the peptidoglycan metabolism of *Escherichia coli*: possible roles of PBP1b and PBP3. J. Bacteriol. **174:**3549–3557.
58. **Wang, L., M. K. Khattar, W. D. Donachie, and J. Lutkenhaus.** 1998. FtsI and FtsW are localized to the septum in *Escherichia coli*. J. Bacteriol. **180:**2810–2816.
59. **Weiss, D. S., J. C. Chen, J.-M. Ghigo, D. Boyd, and J. Beckwith.** 1999. Localization of FtsI (PBP3) to the septal ring requires its membrane anchor, the Z ring, FtsA, FtsQ, and FtsL. J. Bacteriol. **181:**508–520.
60. **Weiss, D. S., K. Pogliano, M. Carson, L.-M. Guzman, C. Fraipont, M. Nguyen-Distèche, R. Losick, and J. Beckwith.** 1997. Localization of the *Escherichia coli* cell division protein FtsI (PBP3) to the division site and cell pole. Mol. Microbiol. **25:**671–681.
61. **Wientjes, F. B., and N. Nanninga.** 1991. On the role of high molecular weight penicillin-binding proteins in the cell cycle of *Escherichia coli*. Res. Microbiol. **142:**333–344.
62. **Yanouri, A., R. A. Daniel, J. Errington, and C. E. Buchanan.** 1993. Cloning and sequencing of the cell division gene *pbpB*, which encodes penicillin-binding protein 2B in *Bacillus subtilis*. J. Bacteriol. **175:**7604–7616.
63. **Yousif, S. Y., J. K. Broome-Smith, and B. G. Spratt.** 1985. Lysis of *Escherichia coli* by β-lactam antibiotics: deletion analysis of the role of penicillin-binding proteins 1A and 1B. J. Gen. Microbiol. **131:**2839–2845.
64. **Yu, X.-C., A. H. Tran, Q. Sun, and W. Margolin.** 1998. Localization of cell division protein FtsK to the *Escherichia coli* septum and identification of a potential N-terminal targeting domain. J. Bacteriol. **180:**1296–1304.